Fine-Tuning of Metallaborane Geometries: Chemistry of Iridaboranes Derived from the Reaction of $[(Cp^*Ir)_2H_xCl_{4-x}]$ ($x = 0-2$; $Cp^* = \eta^5$-C_5Me_5) with $LiBH_4$

Xinjian Lei,* Maoyu Shang, and Thomas P. Fehlner*

Abstract: From reaction of $[(Cp^*Ir)_2H_xCl_{4-x}]$ ($x = 1, 0$) and $LiBH_4$, *arachno*-[{Cp*IrH$_2$}B$_3$H$_7$](**1**) is produced in moderate yield concurrently with [Cp*IrH$_4$]. In contrast, reaction of $[(Cp^*Ir)_2H_2Cl_2]$ with $LiBH_4$ results in *arachno*-[{Cp*IrH}$_2$(μ-H)B$_2$H$_5$] (**3**) in high yield at room temperature but a mixture of **1** and [{Cp*IrH}$_2$(μ-H)BH$_4$] (**2**) at 0 °C. $BH_3 \cdot THF$ converts **1** to *arachno*-[{Cp*IrH}B$_4$H$_9$] (**4**) and **2** to **3** with **1** as a minor product. Further, reaction of **3** with excess of $BH_3 \cdot THF$ results in formation of *nido*-[{Cp*Ir}$_2$-(μ-H)B$_4$H$_7$] (**6**) formed by loss of H_2 from the intermediate *arachno*-[{Cp*IrH}$_2$B$_4$H$_8$] (**5**). Reaction of **1** with $[Co_2(CO)_8]$ permits the isolation of two metallaboranes, *arachno*-[{Cp*Ir(CO)}-B$_3$H$_7$] (**7**) and *nido*-[1-{Cp*Ir}-2,3-Co$_2$-(CO)$_4$(μ-CO)B$_3$H$_7$] (**8**). Treatment of **4** with $[Co_2(CO)_8]$ gives only one single mixed-metal metallaborane *nido*-[1-{Cp*Ir}-2-Co(CO)$_3$B$_4$H$_7$ (**9**) in high yield. Finally, pyrolysis of **8** results in loss of hydrogen and formation of *pileo*-[1-{Cp*Ir}-2,3-Co$_2$(CO)$_5$B$_3$H$_5$] (**10**) with a BH-capped square-pyramidal structure. With kinetic control rational synthesis of a variety metallaboranes has been achieved by varying the number of chlorides in the monocyclopentadienylmetal halide dimer, reaction temperature, types of monoborane, and metal fragment sources.

Keywords: boron · clusters · iridium · metallaboranes · structure elucidation

Introduction

The reaction of a metal chloride with a Group 13 hydride, such as $LiBH_4$ or $LiAlH_4$, constitutes one of the standard procedures to prepare metal hydrides.[1] It is well established that metathesis of Cl^- by a *pseudo* halide, for example BH_4^-, followed by displacement of the Lewis acid, for example BH_3, yields the metal hydride.[2, 3] On the other hand, a metal reagent with more than one chloride can be employed to produce a polyborohydride intermediate, thereby permitting elimination of H_2 with formation of a metallaborane to compete with Lewis acid displacement and metal hydride formation. Indeed, we have demonstrated the reaction of binuclear $[Cp^*MCl_n]$ complexes ($Cp^* = \eta^5$-C_5Me_5) with $LiBH_4$ is a general route to metallaboranes. Detailed investigations of the Co,[4] Rh,[5, 6] Ru,[6] Cr,[7] Mo,[8, 9] and W[10, 11] systems have been reported to date. Metal identity affects products. For example, earlier transition metals facilitate hydrogen loss, leading to highly condensed clusters, such as [{Cp*Re}$_2$B$_7$H$_7$],[12] whereas later transition elements form stable *nido*-metallaboranes, such as 2,4-[{Cp*Co}$_2$B$_3$H$_7$][4] and [1,2-{Cp*Ru}$_2$B$_4$H$_{10}$].[6] Thus, we expect Ir also to exhibit characteristics related to, but different from, those of its Group 9 congeners.

Iridaboranes are known. Mono- and dinuclear iridaboranes have been reported by insertion of metal fragments into known polyborane cages.[13, 14] Examples include *arachno*-[(Ph$_3$P)$_2$(CO)HIrB$_3$H$_7$],[15] *arachno*-[L$_2$(CO)IrB$_4$H$_9$] (L = PMe$_2$Ph, PMe$_3$),[16, 17] *nido*-[(Ph$_3$P)$_2$(CO)IrB$_5$H$_8$],[18] *nido*-[2-{Cp*Ir}B$_4$H$_8$],[19] and the mono-capped *closo*-octahedron [{Cp*Ir}$_2$B$_5$H$_5$][19] plus other mixed iridium–osmium metallaboranes.[20–26] However, the procedures employed involve chromatography of mixtures, and pure compounds are isolated in low yields.

The reaction of $[(Cp^*Ir)_2Cl_4]$ with $NaBH_4$ in alcohol was used by Maitlis et al. to prepare $[(Cp^*Ir)_2HCl_3]$ and $[(Cp^*Ir)_2H_3]PF_6$.[27] Later, Bergman et al. reported that the reaction of $[(Cp^*Ir)_2H_3]PF_6$ with an excess of $LiBH_4$ gives [{Cp*IrH}$_2$(μ-H)(μ-BH$_4$)].[28] Hydrolysis of [{Cp*IrH}$_2$-(μ-H)(μ-BH$_4$)] yields the polyhydride dimer [Cp*IrH$_3$]$_2$. Thus, in contrast to our work on Co[4] and Rh,[6] iridium presented the possibility of examining, not only the chloro complexes, but also the mixed hydride/chloro complexes, that is $[(Cp^*Ir)_2H_xCl_{4-x}]$, $x = 0-2$.[29, 30] The results described below demonstrate a complex, but understandable, competition between H_2 and borane elimination and iridium poly-

[a] Dr. X. Lei, Prof. T. P. Fehlner, Dr. M. Shang
Department of Chemistry and Biochemistry
251 Nieuwland Science Hall
University of Notre Dame
Notre Dame, IN 46556-5670 (USA)
Fax: (+1) 219-631-6652
E-mail: Lei.1@nd.edu
Fehlner.1@nd.edu

  0947-6539/00/0614-2653 $ 17.50+.50/0

borohydride disproportionation, yielding iridaboranes and iridium polyhydrides. Furthermore, the chemistry is elaborated with cluster expansion reactions of these new compounds with borane and metal carbonyl sources.

Results and Discussion

Iridaborane synthesis

***arachno*-[{Cp*IrH$_2$}B$_3$H$_7$] (1)**: The reaction of [(Cp*Ir)$_2$Cl$_4$] with BH_4^- in THF gives a light yellow solution which upon removal of solvents affords a yellow oil. The ^{11}B NMR spectrum indicates that there is only one metallaborane compound **1**. However, the ^{1}H NMR spectrum shows that there are several species in the reaction mixture. The two major compounds have almost identical intensities for the Cp* groups and one of the signals corresponds a known iridium polyhydride monomer, [Cp*IrH$_4$]. A minor compound is the iridium polyhydride dimer [Cp*IrH$_3$]$_2$. [Cp*IrH$_4$] is reported as colorless crystals which can be sublimed at 30–40 °C, while [{Cp*IrH$_3$}$_2$] is orange. Both compounds decompose in the solid state at 50–100 °C.[28, 31] It was hoped that sublimation could be used to remove the [Cp*IrH$_4$] from **1** and that prolonged heating could decompose the [{Cp*IrH$_3$}$_2$]. In fact, sublimation of the yellow oil gives white solids and a yellow residue; however, the ^{11}B NMR spectrum showed that **1** was in the white solid not the yellow residue. The ^{1}H NMR spectrum of the white solids confirmed the presence of **1** and showed only a small amount of [Cp*IrH$_4$].

Recrystallization from hexane gave pure colorless crystals of **1**. The spectroscopic data suggest a seven skeletal electron pair (7-sep) *aracho*-monometallaborane with the molecular formula [{Cp*IrH$_2$}B$_3$H$_7$]. The ^{11}B NMR spectrum reveals two boron environments, one (doublet of triplets) associated with two terminal hydrogen atoms and the other (doublet) with one terminal hydrogen. Both signal patterns are similar to those reported for known 'borallyl' complexes, such as [{Cp*Co(CO)}B$_3$H$_7$][32] and [{(PPh$_3$)$_2$Ir(CO)H}B$_3$H$_7$],[15], and Group 10 tetraborane clusters.[33–38] The IR spectrum also shows the three B–H stretching bands of the 'borallyl' fingerprint.[39] The ^{1}H{selective ^{11}B} NMR experiments further support the proposed structure (Figure 1). Three signals, in the ratio of 1:4:2, are observed for five B-H$_t$ fragments and two B-H-B bridging hydrogens. In the high-field region, a single sharp integral 2H is assigned to the Ir-H$_t$ hydride. Despite many attempts, single-crystal analysis failed due to quick decay of the crystals of **1** in the X-ray beam. Under X-ray irradiation, the colorless crystals became yellow over a period of 10 h. In contrast, the colorless crystals were stable for several days without exposure to the X-ray beam.

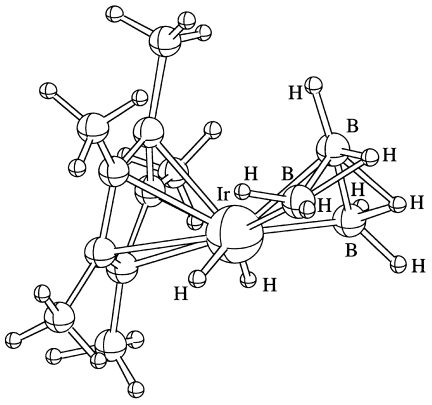

Figure 1. Proposed structure of of **1**.

Note that the reactions of [(Cp*M)$_2$Cl$_n$] with LiBH$_4$ generally give dimetallaboranes in which the number of boron atoms in the dimetallaboranes is directly related to the number of chlorine atoms *n*. Also note that *n* can be less than its value in the actual starting material due to rapid reduction prior to metallaborane formation.[6] Why does the reaction of [(Cp*Ir)$_2$Cl$_4$] with LiBH$_4$ give a monometallaborane instead of dimetallaborane? The proposed explanation is in Scheme 1. Methathesis of Cl^- by BH_4^- is followed by rapid

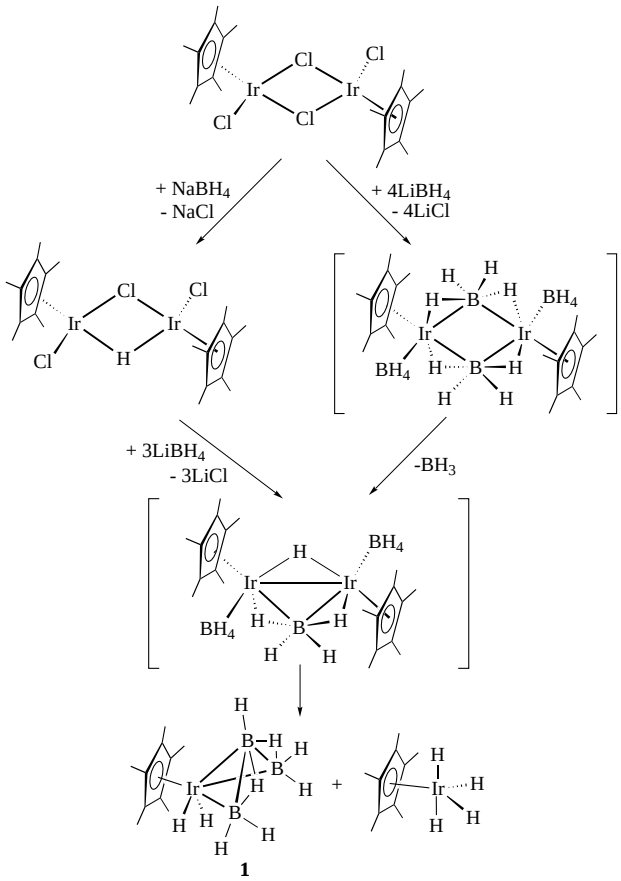

Scheme 1.

loss of one BH_3 group to give [(Cp*Ir)$_2$(μ-H)(BH$_4$)$_3$]. Before additional loss of borane, it dissociates to yield **1** and its coproduct [Cp*IrH$_4$]. Visual observation shows that dark red [(Cp*Ir)$_2$HCl$_3$] is not present in large quantities during the reaction. The reaction of [(Cp*Ir)$_2$HCl$_3$] with LiBH$_4$ yields the same products, thereby supporting the above hypothesis. Formation of **1** is presumably driven by the simultaneous formation of stable [Cp*IrH$_4$]. The minor product [{Cp*IrH$_3$}$_2$] most likely arises from decomposition of [(Cp*Ir)$_2$(μ-H)(BH$_4$)$_3$].

0947-6539/00/0614-2654 $ 17.50+.50/0 *Chem. Eur. J.* **2000**, *6*, No. 14

***arachno*-[{Cp*IrH}$_2$(μ-H)BH$_4$] (2)**: If the reaction path in Scheme 1 is correct, treatment of [(Cp*Ir)$_2$H$_2$Cl$_2$] with LiBH$_4$ can only give [(Cp*Ir)$_2$(μ-H)$_2$(BH$_4$)$_2$] which should not yield the same products as those from the reaction with [(Cp*Ir)$_2$Cl$_4$] or [(Cp*Ir)$_2$HCl$_3$]. The reaction of [(Cp*Ir)$_2$H$_2$Cl$_2$] with LiBH$_4$ in THF at 0 °C gives a reddish solution. The ^{11}B NMR spectrum indicates the presence of **1** and the known compound, [{Cp*IrH}$_2$(μ-H)(μ-BH$_4$)] (**2**) in a ratio of 1:1. As already mentioned, **2** was prepared earlier from the reaction of [(Cp*Ir)$_2$H$_3$]PF$_6$ with LiBH$_4$.[28] The ^{1}H NMR spectrum shows that [Cp*IrH$_4$] is present as well. The origin of **1**, **2**, and [Cp*IrH$_4$] can best be explained by the reaction pathway in Scheme 2. A rapid metathesis of Cl$^-$ by BH$_4^-$ gives an intermediate [(Cp*Ir)$_2$(μ-H)$_2$(BH$_4$)$_2$] which undergoes bimolecular BH$_3$ exchange to give **2** and [(Cp*Ir)$_2$(μ-H)(BH$_4$)$_3$] which is the intermediate in Scheme 1. The latter dissociates to provide **1** and [Cp*IrH$_4$]. The color of the reaction was reddish consistent with the ^{1}H NMR spectrum of the reaction mixture which indicated the presence of a small amount of dark red [{Cp*IrH$_2$}$_2$]. [40]

***arachno*-[{Cp*IrH}$_2$(μ-H)B$_2$H$_5$] (3)**: When the reaction of [(Cp*Ir)$_2$H$_2$Cl$_2$] with LiBH$_4$ in THF is carried out at room temperature, a single metallaborane is produced in high yield, accompanied by a small amount of **2**. The new compound **3** is isolated in crystalline form and the ^{11}B NMR spectrum shows two boron environments with a ratio of 1:1. The proton NMR spectrum exhibits two kinds of Cp* groups and five hydrides in the high-field region. The mass spectral data suggest that **3** has the molecular formula [(Cp*Ir)$_2$B$_2$H$_8$]. The solid-state structure determination reveals that the new compound consists of a dinuclear [(Cp*IrH)$_2$(μ-H)] fragment bridged asymmetrically by a B$_2$H$_5$ ligand (Figure 2). The same coordination mode of the B$_2$H$_5$ fragment has been shown in other compounds such as [{Cp*Co}$_2$(μ-PPh$_2$)B$_2$H$_5$][41] and [Pt$_2$(PMe$_2$Ph)$_2$(B$_2$H$_5$)(B$_6$H$_9$)].[42] Compounds **3** and **1** are related in that replacement of a BH vertex of **1** by an isolobal Cp*Ir fragment generates **3**. Both belong to the family of metallaborane analogues of *arachno*-tetraborane(10) in that one or two Cp*Ir fragments subrogate isolobal BH moieties.

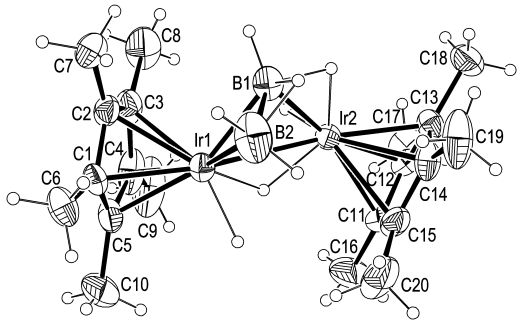

Figure 2. Molecular structure of **3**. Selected bond lengths [Å] and angles [°]: Ir1–Ir2 2.8227(8), Ir1–B1 2.169(13), Ir1–B2 2.23(2), Ir2–B1 2.178(14), B1–B2 1.83(2); B1-Ir1-B2 49.2(6), B2-Ir1-Ir2 80.1(4), B1-Ir2-Ir1 49.4(3), B2-B1-Ir1 67.1(7), B2-B1-Ir2 109.6(9), Ir1-B1-Ir2 81.0(5), B1-B2-Ir1 63.7(6).

As has been observed earlier in reactions of borane (and other systems), a unimolecular reaction is associated with a larger $\Delta S^{\ddagger}$ and $\Delta H^{\ddagger}$ relative to a bimolecular reaction. Thus, the former, H$_2$ elimination from [(Cp*Ir)$_2$(μ-H)$_2$(BH$_4$)$_2$] yielding **3**, is favored at higher temperatures and the latter, borane exchange leading to **1** and **2**, at lower temperatures (Scheme 2). Importantly, a separate experiment shows that **3** can be obtained from the reaction of **2** with an excess of BH$_3$·THF accompanied by a small amount of **1** and [Cp*IrH$_4$]. This represents the first example of conversion of an *arachno*-M$_2$B to an *arachno*-M$_2$B$_2$ cluster.

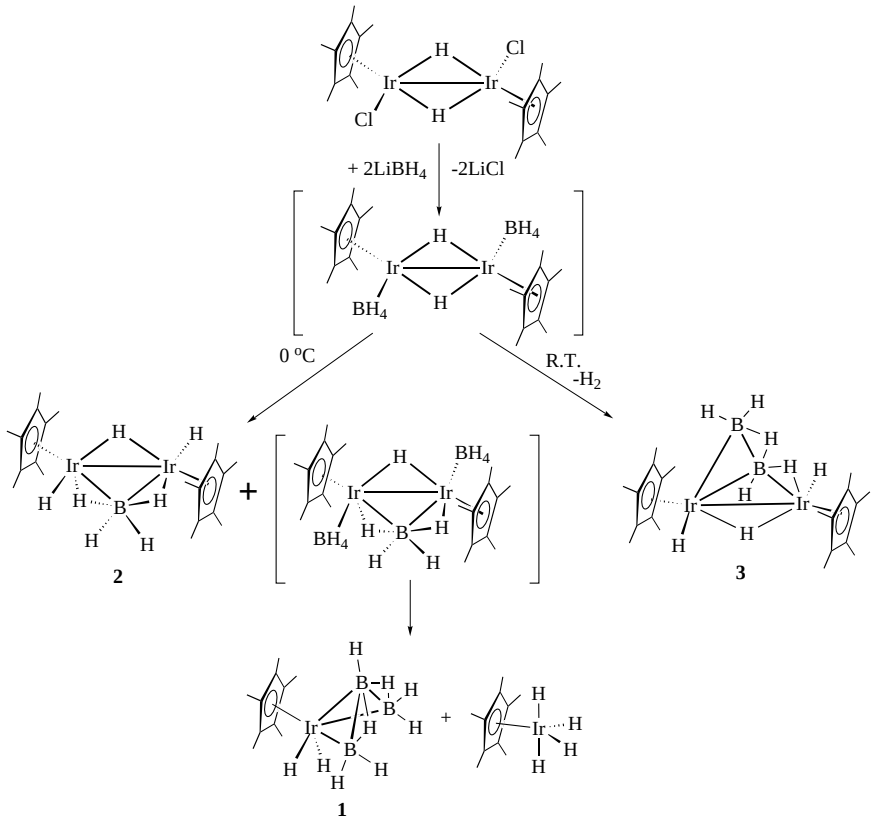

Scheme 2.

Monometallaborane versus dimetallaborane: Reaction pathways for the formation of **1**–**3** are given in Schemes 1 and 2. Owing to the unique properties of Ir, the chemistry observed is significantly different from that of the other Group 9 metals, Co[4] and Rh.[6] Unlike Co and Rh, which yield [{Cp*M}$_2$B$_2$H$_6$]

from the reaction with $LiBH_4$, reactions of $[(Cp^*Ir)_2Cl_4]$ and $[(Cp^*Ir)_2HCl_3]$ with $LiBH_4$ yield **1** plus co-product $[Cp^*IrH_4]$, whereas reaction of $[\{Cp^*Ir\}_2H_2Cl_2]$ with $LiBH_4$ at room temperature results in formation of **3**. Consistent with their differing electron counts, the compounds $[\{Cp^*M\}_2B_2H_6]$ (M = Co, Rh) adopt a tetrahedral geometry, while **3** is a butterfly shape. Reaction of $[(Cp^*M)_2Cl_n]$ with $BH_3\cdot THF$ (Co and Rh) with elimination of BH_2Cl leads directly to a *nido*-$[\{Cp^*M\}_2B_3H_7]$ cluster, whereas the same reaction with $[(Cp^*Ir)_2H_xCl_{4-x}]$ results in an unseparable mixture of **1**, **2**, and **3**. Isolation of **1**–**3** demonstrates that the fate of the polyborohydride dimers is dependent on the metal centers, that is, for the first- and second-row metals, rapid loss of hydrogens to form *nido*-dimetallaboranes is preferred, whereas the third-row metal exhibits a competitive chemistry undergoing either dissociation to give monometallaboranes, elimination of H_2 to give *arachno*-dimetallaboranes, or loss of BH_3 to generate metal hydrides.

Controlled cluster expansion

Addition of a BH fragment to *arachno*-[{Cp*IrH$_2$}B$_3$H$_7$] (1): The reaction of **1** with $BH_3\cdot THF$ gives a single compound in high yield. Like **1**, sublimation affords pure colorless crystals of **4.** The ^{11}B NMR spectrum shows two boron environments with a ratio of 1:1. The proton NMR spectrum exhibits two kinds of B-H-B with a ratio of 1:2, plus one terminal Ir–H in the high-field region. The mass spectral data suggest addition of one BH fragment to **1**, that is, $[\{Cp^*IrH\}B_4H_9]$. Again, a solid-state structure determination was frustrated by rapid decay upon exposure to the X-ray beam plus a disorder problem. However, on the basis of spectroscopic data, this compound is the 8-sep *arachno*-monometallapentaborane $[\{Cp^*IrH\}B_4H_9]$ (**4**) (Figure 3).

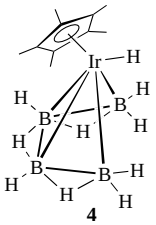
4

The formation of **4** is the first example of conversion of an *arachno*-monometallatetraborane into an *arachno*-monometallapentaborane. Other known *arachno*-Group 9 monometallapentaboranes include *arachno*-1-$\{Cp^*CoH\}B_4H_9$, isolated in low yield from the reaction of $[Cp^*CoCl]$ with $BH_3\cdot THF$,[4] $[Ir\{P(CH_3)_2C_6H_5\}_2(CO)B_4H_9]$, obtained by the reaction of $K[B_4H_9]$ with *trans*-$[IrCl\{P(CH_3)_2C_6H_5\}_2(CO)]$,[16] and *nido*-[2-$\{Cp^*Ir\}B_4H_8$] from reaction of $[(Cp^*Ir)_2Cl_4]$ with $Na_2B_5H_9$.[19]

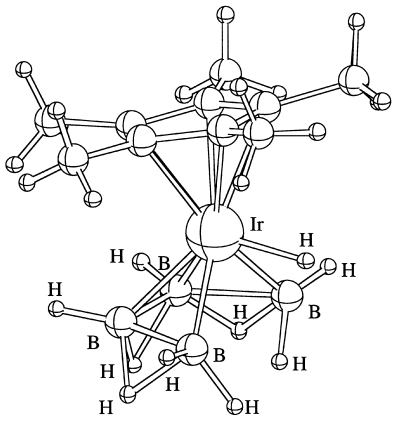
Figure 3. Proposed structure of **4**.

Addition of BH fragments to *arachno*-[{Cp*IrH}$_2$(μ-H)B$_2$H$_5$] (3): The ^{11}B NMR spectrum shows the reaction of pure **3** with $BH_3\cdot THF$ in hexane results in two boron-containing compounds. Luckily, one of them had lower solubility than the other in hexane and was crystallized out at $-40\,^\circ C$. The ^{11}B NMR spectrum shows two boron environments with a ratio of 1:1, and the proton NMR spectrum exhibits one kind of Cp* ligand, two equivalent B-H-B and two equivalent Ir-H terminal hydrogens. The mass spectral data suggest a molecular formula, $[\{Cp^*IrH\}_2B_4H_8]$. On the basis of spectroscopic data, the compound is formulated as a 9-sep, six-vertex, *arachno*-dimetallahexaborane, demonstrating that cluster expansion by the formal insertion of two BH fragments into **3** has taken place. According to the known structure of B_6H_{12}, there are three possible structures for a hexaborane(12) analogue in which two BH vertices are replaced by two Cp*Ir fragments which are consistent with the solution NMR data. The solid-state structure shows the new iridaborane to be *arachno*-[2,5-$\{Cp^*IrH\}_2B_4H_8$] (**5**) (Figure 4). The molecule is

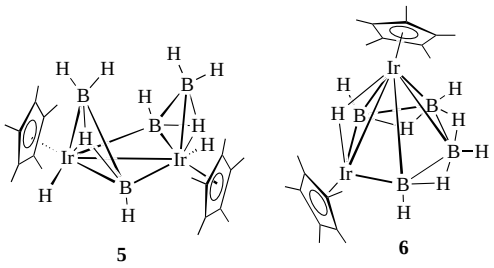
5 **6**

located on a crystallographic twofold axis, resulting in equivalent Cp* environments in good agreement with the solution NMR data. Compound **5** represents the first example of a metallaborane analogue of hexaborane(12). The structural metrics of **5** are comparable to those of **3**.

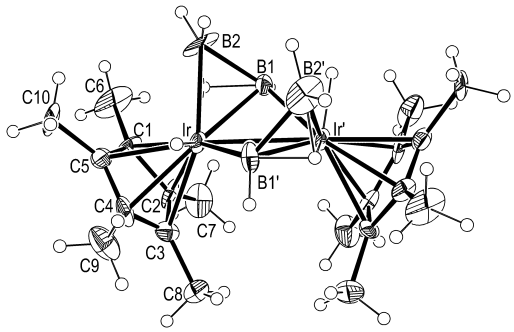
Figure 4. Molecular structure of **5**. Selected bond lengths [Å] and angles [°]: Ir–Ir′ 2.7814(9), Ir–B1 2.160(14), Ir–B1′ 2.18(2), Ir–B2 2.19(2), B1–B2 1.85(3), B1–Ir′ 2.18(2); B1-Ir-B1′ 93.2(7), B1-Ir-B2 50.2(8), B1′-Ir-B2 99.3(7), B1-Ir-Ir′ 50.5(4), B1′-Ir-Ir′ 49.8(4), B2-Ir-Ir′ 87.2(6), B2-B1-Ir 65.8(9), B2-B1-Ir′ 118.0(11), Ir-B1-Ir′ 79.7(5).

0947-6539/00/0614-2656 $ 17.50+.50/0 *Chem. Eur. J.* **2000**, *6*, No. 14

If the reaction of **3** with excess of $BH_3 \cdot THF$ in THF is carried out over a longer period of time at 65 °C, only a single metallaborane is produced. The same metallaborane is produced by simply heating **5**. The ^{11}B NMR spectrum shows two boron environments with a ratio of 1:1 and the proton NMR spectrum reveals two kinds of Cp* ligand, two kinds of B-H-B with a ratio of 1:2, and one Ir-H terminal hydrogen. The mass spectral data suggest a molecular formula, $[\{Cp^*Ir\}_2B_4H_8]$. On the basis of spectroscopic data, this compound is an 8-sep, six-vertex, *nido*-dimetallahexaborane. A solid-state structure determination (Figure 5) shows that

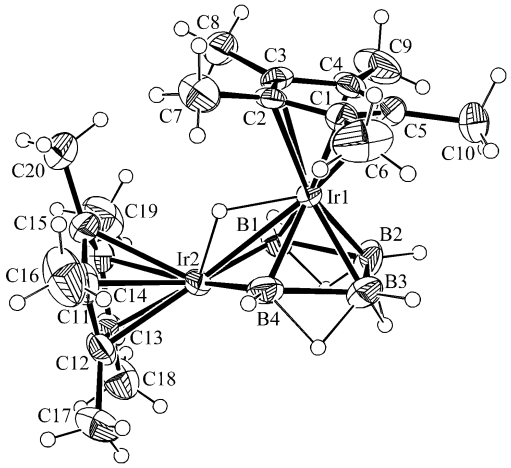

Figure 5. Molecular structure of **6**. Selected bond lengths [Å] and angles [°]: Ir1–Ir2 2.7386(7), Ir1–B2 2.088(13), Ir1–B3 2.106(13), Ir1–B1 2.118(11), Ir1–B4 2.120(13), B1–B2 1.869(19), B2–B3 1.83(2), B3–B4 1.87(2); B2-Ir1-B3 51.9(6), B2-Ir1-B1 52.8(6), B3-Ir1-B1 89.6(6), B2-Ir1-B4 89.6(6), B3-Ir1-B4 52.4(6), B4-Ir2-B1 90.4(6), B4-Ir2-Ir1 50.1(4), B1-Ir2-Ir1 50.0(3), B2-B1-Ir2 114.9(9), B3-B2-B1 106.9(9), B2-B3-B4 106.5(9), B3-B4-Ir2 115.1(9).

the new cluster is *nido*-[1,2-$\{Cp^*Ir\}_2(\mu$-H)B_4H_7] (**6**), in which the core geometry and the skeletal hydrogen atom positions are in full accord with the solution NMR data. Compound **6** is a dimetallahexaborane analogue of B_6H_{10} in which the apical BH and a basal BH are subrogated by isolobal Cp*Ir fragments. Compound **6** is the second structurally characterized dimetallahexaborane. The first is $[\{Cp^*Ru\}_2(\mu$-H)$B_4H_9]$.[6] Interestingly, **6** is the fourth member of the series of compounds $[\{Cp^*M\}_2B_4H_8]$, M = Cr,[43] Re,[44] Ru,[6] Ir,[30] possessing identical compound stoichiometries but different metal identities. Going from early to later transition metal elements, the structure motif changes from condensed to open clusters (bicapped tetrahedron for Cr and Re, monocapped square pyramid for Ru, and pentagonal pyramid for Ir).

The explanation of the cluster expansion from **3** to **5**, to **6** is straightforward. Addition of BH_3 to **3**, followed by loss of H_2 gives a putative *arachno*-$[\{Cp^*IrH\}_2B_3H_7]$ species, a dimetallaborane analogue of pentaborane(11). The structure of **4** constitutes a monometallaborane model for it, that is, replacement of a BH fragment at the 3-position of **4** by Cp*Ir yields the proposed intermediate. Subsequently, a second BH_3 is inserted into $[\{Cp^*IrH)_2B_3H_7]$ with loss of H_2 to give **5.** This in turn slowly eliminates H_2 to yield **6**. Conversion of **5** to **6** constitutes the second example of an *arachno* → *nido* transformation by dihydrogen loss in the iridaborane system and suggests that such a process becomes more facile the higher the B/Ir ratio. As with the ruthenium analogue, *nido*-$[\{Cp^*RuH\}_2B_4H_8]$,[6] **6** does react with $[Co_2(CO)_8]$ but yields only small amounts of boron-containing species. Compound **6** is stable at 100 °C overnight.

Stepwise addition of a BH fragment: As a general rule, reaction of dimeric monocyclopentadienylmetal chlorides with boranes yields dimetallaboranes as the major products, but the number of BH vertices in the cluster depends on the metal elements and the boranes used, for example, M_2B_n: Rh, $n = 2$;[6] Co,[4] Rh, [6] Ru,[6] $n = 3$; Cr,[43] $n = 4$, Mo,[9] W,[10] $n = 5$; Re,[12] $n = 7$. A stepwise build-up of M_2B_n from $\{Cp^*M\}_2$ fragments is a chemist's ideal. We have almost fulfilled the dream and have demonstrated examples of cluster expansion from M_2B_2 to M_2B_3 for Rh, M_2B_3 to M_2B_4 for Ru, and M_2B_4 to M_2B_5 for Cr . In the present work, in addition to expansion of Ir_2B_2 to Ir_2B_4, presumably through Ir_2B_2 to Ir_2B_3 and then Ir_2B_3 to Ir_2B_4, we have established for the first time the Ir_2B to Ir_2B_2 step. This is summarized in Scheme 3 where the metals on each arrow refer to the metals for which examples of the cluster expansion reaction have been chemically observed.

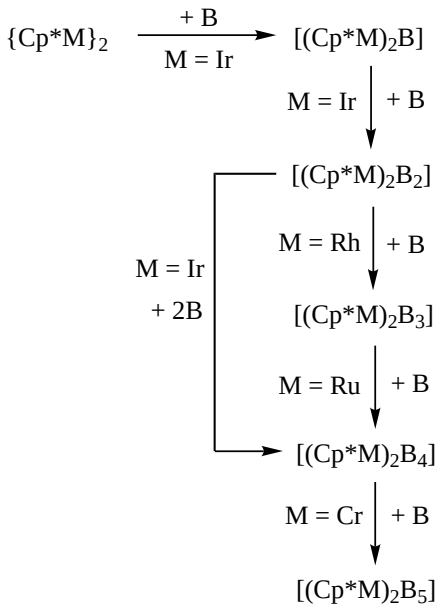

Scheme 3.

Addition of cobalt carbonyl fragments to *arachno*-$[\{Cp^*IrH_2\}B_3H_7]$ (1): The reaction of **1** with an excess of $[Co_2(CO)_8]$ gives a brown solution. The ^{11}B NMR spectra indicate that there are two new metallaborane compounds formed. After work-up, the major one was isolated as colorless needles in good yield and it had the characteristic "borallyl" fingerprints in the ^{11}B NMR and IR spectra. The mass spectral data suggest that two hydrogen atoms in **1** are replaced by one carbonyl ligand, giving a formula $[\{Cp^*Ir(CO)\}B_3H_7]$ (**7**) , that is, **1** with the two Ir-H terminal hydrogens replaced by CO. The solid-state structure deter-

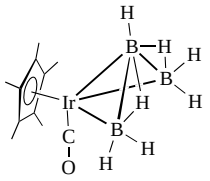

7

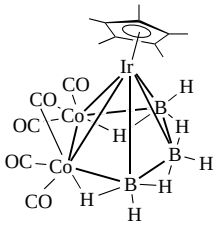

8

mination (Figure 6) is fully consistent with the NMR data. It constitutes the second structurally characterized "borallyl" species with the general formula $[\{Cp^*M(CO)\}B_3H_7]$ (M = Co, Ir).[32] Attempts to prepare **7** by the direct reaction of **1** with carbon monoxide at room temperature or higher temperatures failed. Consequently, it must result from the reaction of **1** with $[Co_2(CO)_8]$. Compound **7** is thermally stable up to over 100 °C in solution.

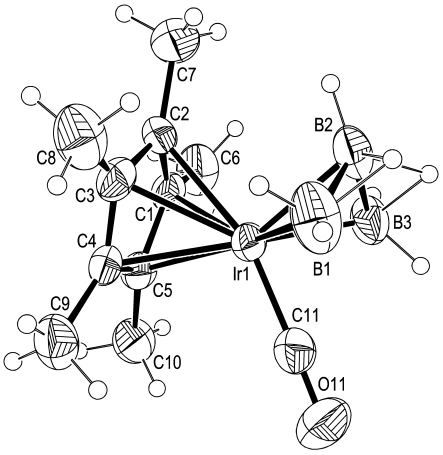

Figure 6. Molecular structure of **7**. Selected bond lengths [Å] and angles [°]: Ir1–C11 1.829(17), Ir1–B2 2.147(17), Ir1–B3 2.170(18), Ir1–B1 2.236(19), B1–B2 1.87(3), B2–B3 1.82(3), C11–O11 1.182(18); C11-Ir1-B2 104.6(7), C11-Ir1-B3 83.0(8), B2-Ir1-B3 49.8(7), B2-Ir1-B1 50.4(8), B3-Ir1-B1 89.0(8), B2-B1-Ir1 62.3(8), B3-B2-B1 113.9(15), B3-B2-Ir1 65.8(8), B1-B2-Ir1 67.3(8), B2-B3-Ir1 64.4(8).

A minor product from the reaction of **1** with an excess of $[Co_2(CO)_8]$ can be isolated as black crystals after removal of **7** from the mother solution. Spectroscopic data suggest addition of a $\{Co_2(CO)_5\}$ fragment accompanied by the loss of hydrogen. A solid-state structure determination (Figure 7) showed that the new compound is an 8-sep trimetallic cluster, *nido*-[1-{Cp*Ir}-2,3-$Co_2(CO)_4(\mu$-CO)B_3H_7] (**8**), fully consistent with the solution NMR and IR data. Compound **8** represents the second structurally characterized trimetal analogue of B_6H_{10} in which an apical and two adjacent basal BH fragments are subrogated by metal fragments as in *nido*-[1-{Cp*Ru}-2-{Cp*RuCO}-3-$Co(CO)_2(\mu_3$-CO)B_3H_6].[6] The open pentagonal face consists of two $Co(CO)_2$ fragments bridged by the fifth CO ligand and three BH groups, resulting in a virtual mirror plane for **8** passing through the middle of Co–Co bond and B2. As with B_6H_{10}, the four *endo*-hydrogen atoms bridge four edges of the pentagonal face. Thus, **8** is an exact metallaborane analogue of hexaborane(10) in terms of

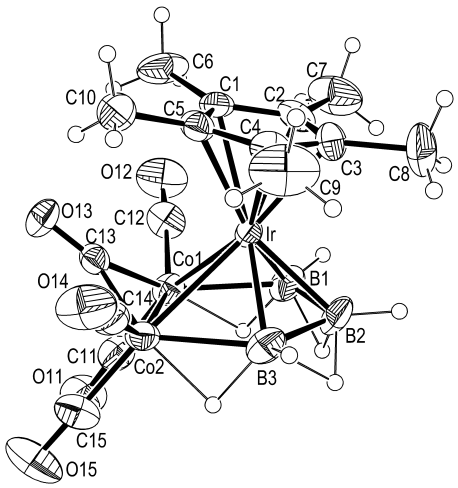

Figure 7. Molecular structure of **8**. Selected bond lengths [Å] and angles [°]: Ir–Co2 2.5701(11), Ir–Co1 2.5828(17), Co1–Co2 2.4406(18), Ir–B2 2.117(9), Ir–B1 2.137(9), Ir–B3 2.141(10), Co1–B1 2.170(11), Co2–B3 2.172(11), B1–B2 1.824(16), B2–B3 1.789(18), Co1–C11 1.766(10), Co1–C12 1.790(10), Co1–C13 1.881(7), Co2–C13 1.888(8), Co2–C14 1.780(10), Co2–C15 1.766(10); Co2-Ir-Co1 56.54(5), Co2-Co1-Ir 61.47(4), B2-Ir-B1 50.8(4), B2-Ir-B3 49.7(5), B1-Ir-B3 87.0(4), B2-Ir-Co2 93.7(3), B1-Ir-Co2 94.6(3), B3-Ir-Co2 54.0(3), B2-Ir-Co1 92.9(3), B1-Ir-Co1 53.7(3), B3-Ir-Co1 92.5(3), B1-Co1-Co2 97.5(3), B3-Co2-Co1 95.8(3), B2-B1-Co1 117.6(6), B3-B2-B1 109.1(7), B2-B3-Co2 119.8(6).

structural motif. Importantly, **8** can also be viewed as an analogue of iridacene as the five-membered ring Co_2B_3 is planar with the mean deviation from the least square plane being 0.02 Å and the dihedral angle between the Cp* and Co2B3 planes only 11.7(4)°. The $Co_2(CO)_5B_3H_7$ fragment represents the second example of a metallocyclic aromatic ring containing no carbon. The first one is a six-membered ring $[Co_2(CO)_5B_4H_4]$ observed in $[\{Cp^*Re\}_2Co_2(CO)_5B_4H_4]$.[44]

Metal fragment addition to *arachno*-[{Cp*IrH}B_4H_9] (4): The reaction of **4** with an excess of $[Co_2(CO)_8]$ gave a single metallaborane in good yield. The spectroscopic data showed the addition of the fragment $Co(CO)_3$ and the loss of three hydrogen atoms, suggesting a six-vertex, 8-sep cluster compound. The *nido* cluster structure suggested by the NMR data was confirmed by a solid-state structure analysis as *nido*-[1-{Cp*Ir}-2-$Co(CO)_3B_4H_7$] (**9**) (Figure 8). The $Co(CO)_3$ fragment formally replaces three *endo* hydrogens which are lost in the form of $HCo(CO)_4$ (^{1}H NMR) and H_2 gas. The Cp*Ir retains an apical position, while the $Co(CO)_3$ fragment occupies the basal position and is connected directly to two boron and one Ir atoms. There are three B-H-B bridging hydrogen atoms on the open pentagonal CoB_4 face, resulting in a virtual mirror plane passing through the Ir–Co edge and bisecting the B2–B3 edge. The five-membered CoB_4 ring, constituting the pentagonal face, is almost planar with the

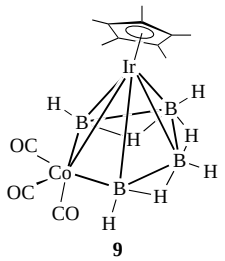

9

0947-6539/00/0614-2658 $ 17.50+.50/0 *Chem. Eur. J.* **2000**, *6*, No. 14

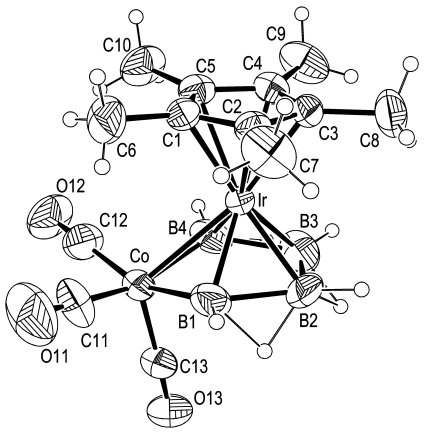

Figure 8. Molecular structure of **9**. Selected bond lengths [Å] and angles [°]: Ir–B1 2.065(9), Ir–B4 2.068(9), Ir–B3 2.095(10), Ir–B2 2.109(10), Ir–Co 2.6167(9), Co–B1 2.043(9), Co–B4 2.045(9), B1–B2 1.807(17), B2–B3 1.78(2), B3–B4 1.856(18), Co–C11 1.773(9), Co–C12 1.797(9), Co–C13 1.776(8); B1-Ir-B4 88.8(4), B1-Ir-B3 87.7(5), B4-Ir-B3 53.0(5), B1-Ir-B2 51.3(5), B4-Ir-B2 89.8(6), B3-Ir-B2 50.1(7), B1-Ir-Co 50.1(3), B4-Ir-Co 50.1(2), B3-Ir-Co 87.0(3), B2-Ir-Co 87.0(3), B1-Co-B4 90.0(4), C11-Co-Ir 110.7(3), C13-Co-Ir 120.5(2), C12-Co-Ir 110.6(3), B2-B1-Co 116.4(8), B3-B2-B1 107.0(7), B2-B3-B4 108.4(8), B3-B4-Co 113.6(8), B3-B4-Ir 64.3(5), Co-B4-Ir 79.0(3).

mean deviation from the least square plane being 0.12 Å. The Cp* and CoB_4 planes are parallel to each other with a dihedral angle of 5.1(5)°. Thus, **9** can also be viewed as an analogue of iridacene if the metallocylic fragment $Co(CO)_3B_4H_7$ is regarded as an inorganic analogue of the η^5-C_5H_5 ligand. Compound **9** represents the first structurally characterized heterobimetallahexaborane analogue of B_6H_{10} and is an isomeric form of the nido-[4-{(*p*-cym)Ru}-5-{$(Ph_3P)_2$(CO)Os}B_4H_8] (*p*-cym = [1-Me-4-(PrC_6H_4)-*i*Pr) in which the two metal atoms occupy two adjacent basal positions.[45] A ^{11}B NMR study shows that **9** is stable at 100 °C and inert to phosphine ligands, such as PPh_3.

Group 9 metallaborane reactivities: We have previously reported the reactivity of *nido*-[{Cp*M}$_2B_2H_6$] (M = Co, Rh) and their derivatives towards the test reagents, $BH_3 \cdot THF$, [$Co_2(CO)_8$], and [$Fe_2(CO)_9$].[4, 6] Vertex exchange and cluster degradation reaction for Co and addition of a BH fragment and metal carbonyl fragments for Rh have been observed. These observations on Co and Rh can now be compared and contrasted with those found for Ir.

Compounds **1** and **3** both adopt a butterfly structure and can be viewed as metallaborane analogues of tetraborane(10). Their reactivity towards the same test reagents reveals another aspect of the reactivity of Group 9 metallaboranes, that is the number of metal fragments in a given structure type. Iridaborane clusters display a richer chemistry than its congeners. Compound **1** undergoes facile cluster expansion reactions with borane and [$Co_2(CO)_8$] to yield analogous *arachno*-monoiridapentaborane (**4**), *arachno*-monoiridatetraborane (**7**), and *nido*-trimetallahexaborane (**8**) clusters. In contrast to **1**, **3** undergoes cluster expansion only with borane to sequentially give the *arachno*- and *nido*-clusters **5** and **6**.

As with reactions of Co and Rh derivatives with $Co_2(CO)_8$, a reaction pathway via the [$Co(CO)_4$]$^\cdot$ radical is likely. The reaction of **1** with [$Co_2(CO)_8$] may first generate [{Cp*IrH}-$Co(CO)_4B_3H_7$] by hydrogen extraction from **1** by [$Co(CO)_4$]$^\cdot$ to give [{Cp*IrH}B_3H_7]$^\cdot$ and [$HCo(CO)_4$] (observed in the ^{1}H NMR spectrum) followed by addition of [$Co(CO)_4$]$^\cdot$ to the radical. Then, loss of [$HCo(CO)_4$] and addition of CO ligand gives **7**. On the other hand, in the presence of high concentrations of [$Co(CO)_4$]$^\cdot$, repetition of the above procedure could give a second intermediate, [{Cp*Ir}($Co(CO)_4)_2B_3H_7$], which upon loss of CO groups with formation of Co–Co and B–Co bonds forms **8**.

Dehydrogenation

***arachno*-[{Cp*IrH}$_2$(μ-H)B_2H_5] (3)**: The observed M_2B_2 form for Co and Rh is *nido*-[{Cp*M}$_2B_2H_6$];[6] however, attempts to convert **3** to [{Cp*Ir}$_2B_2H_6$] failed as **3** decomposed before H_2 was lost. However, such *arachno* → *nido* transitions with loss of H_2 have been observed in larger iridaborane systems, for example the conversion of *arachno*-[(CO)($PMe_3)_2$HIrB_8H_{12}] to *nido*-[(CO)($PMe_3)_2$IrB_8H_{11}] under mild thermolysis or UV photolysis.[46]

***arachno*-[{Cp*IrH}B_4H_9] (4)**: The analogue of **4**, *arachno*-[1-{Cp*CoH}B_4H_9], readily converts into *nido*-[1-{Cp*Co}B_4H_8] upon heating at 80 °C by loss of H_2.[4] Although *nido*-[2-{Cp*Ir}B_4H_8] is known,[19] attempts to convert **4** to a *nido*-[1-{Cp*Ir}B_4H_8] failed as **4** was stable up to 100 °C and heating at over 100 °C led to decomposition. The difference in stability is probably due to the stronger affinity of hydrogen for Ir versus Co.

***nido*-[1-{Cp*Ir}-2,3-$Co_2(CO)_4$(μ-CO)B_3H_7] (8)**: The pyrolysis of **8** results in high-yield conversion to a new metallaborane. The mass spectrometric data show the loss of two hydrogen atoms from **8**, presumably as H_2 gas and the IR spectrum indicates the retention of the $Co_2(CO)_5$ fragment of **8** but without any bridging CO bands. The ^{11}B NMR spectrum indicates that the plane of symmetry in **8** is lost, that is, there are three boron environments and that giving rise to the signal at $\delta = 103.8$ is likely a boron capping a trimetal face. This suggests that the product is *pileo*-[1-{Cp*Ir}-2,3-Co_2-$(CO)_5B_3H_5$] (**10**), an analogue of *pileo*-[1,2,3-{Cp*Ru}$_3$(μ-H)B_3H_7].

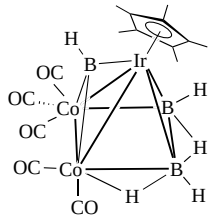

10

A solid-state structure determination reveals that there are four molecules in the asymmetrical unit (Figure 9). Each consists of a [1,2,3-{Cp*Ir}$Co_2(CO)_5B_2H_4$] square pyramid with the trimetal face capped by the third BH fragment. The open square face formed by one $Co(CO)_3$ fragment, one $Co(CO)_2$ fragment, and two BH groups has two *endo* bridging hydrogens, making the compound chiral. All the carbonyl groups are terminal, fully consistent with the IR data. Unlike *pileo*-[1,2,3-{Cp*Ru}$_3$(μ-H)B_3H_7], the core structure of **10** exhibits considerable distortion. The Ir–B distance (2.181(3) Å) of the basal boron atom associated with two bridging hydrogen atoms is significantly longer than that of **10**

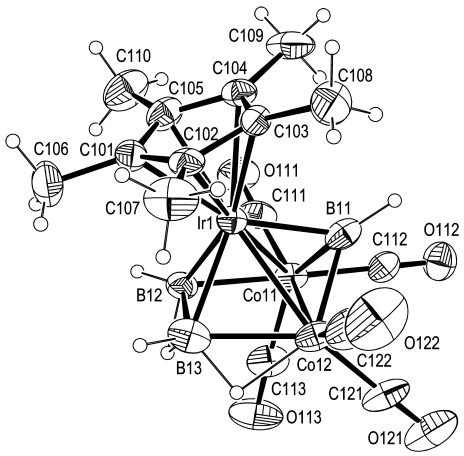

Figure 9. Molecular structure of **10**. Selected bond lengths [Å] and angles [°]: Ir1–Co12 2.5173(14), Ir1–Co11 2.5901(13), Co11–Co12 2.5250(18), Ir1–B11 2.028(13), Ir1–B12 2.051(12), Ir1–B13 2.177(13), Co11–B11 2.119(11), Co11–B12 2.136(13), Co12–B11 1.943(13), Co12–B13 2.206(16), Co11–C(113) 1.760(12), Co11–C111 1.778(11), Co11–C112 1.796(12), Co12–C122 1.745(13), Co12–C121 1.752(13); B11-Ir1-B12 104.3(5), B12-Ir1-B13 50.6(5), B11-Ir1-Co12 49.2(3), B12-Ir1-Co11 53.3(4), Co12-B11-Co11 76.7(4), B11-Co11-B12 98.4(5), B11-Co11-Co12 48.5(3), B12-Co11-Co12 78.9(3), B(13)-Co(12)-Co(11) 81.9(3), B13-B12-Co11 103.7(8), B12-B13-Co12 95.2(7).

(2.13(1) Å), while the Ir–B bonds (2.03(1) Å) of the capped boron atom are much shorter. The Ir–Co distances also fall into two groups: short (2.519(1) Å) for those connected to the $Co(CO)_2$ fragment and long (2.591(1) Å) for those associated with the $Co(CO)_3$ groups. The latter are comparable to those (2.576 Å) in **8**. The Co–Co distances (2.523(1) Å) are significantly longer than that (2.440(1) Å) in **8**. Compound **10** represents the second example of a capped trimetallapentaborane to be reported. The first is *pileo*-[1,2,3-{Cp*Ru}$_3$(μ-H)B_3H_7] isolated as a minor product in the reaction of [$(Cp^*Ru)_2Cl_4$] with $LiBH_4$.[47]

Summary

A rational synthetic route to *arachno*-IrB_3 and *arachno*-Ir_2B_2 clusters in good yields has been developed by the reaction of $LiBH_4$ with [$(Cp^*Ir)_2H_xCl_{4-x}$] ($x = 0, 1, 2$). It has been shown that the products obtained are directly related to the number of chlorides in the monocyclopentadienyliridium dimer and that it is possible to engineer the cluster geometry by retaining the dimeric framework and changing the number of chlorides by introducing hydrides.

We have demonstrated the rational cluster expansion of mono- and diiridaborane with borane and metal carbonyl fragments. Our observations in this Ir system, as well as other related systems, suggest that the metal fragment provides an electron-rich site for electrophilic attack, promoting addition of BH_3 and metal carbonyl fragments to metallaborane clusters.

One of the fascinating aspects of metallaborane chemistry is its close connection with organometallic chemistry. For example, existence of isoelectronic pairs such as [$(CO)_4FeB_2H_5$]$^-$ versus [$(CO)_4Fe(\eta^2$-$C_2H_4)$], [{CpCo}B_4H_8] versus [{Cp*Co}(η^4-C_4H_4)], and [CpFeCp] versus [$B_5H_{10}FeB_5H_{10}$].[48] Compounds **5** and **6** provide another connection. Transition metal compounds promote the conversion of two alkynes into metallacyclopentadienes, so-called metalloles.[49, 50] For the formation of cobaltoles, coordination of alkynes followed by oxidative cyclization of two alkynes is the suggested route (Scheme 4).[51] Note then that **5** contains

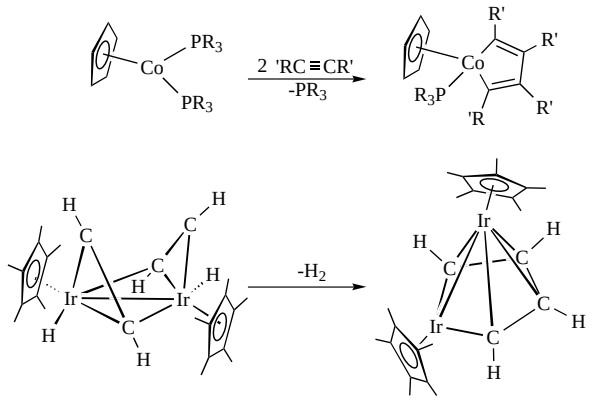

Scheme 4.

two separated B_2H_4 fragments which are isoelectronic with C_2H_2 and that mild thermolysis of **5** results in H_2 elimination to give **6**. The open pentagonal face of **6** can be viewed as an analogue of a metallole [{Cp*Ir}C_4H_4], that is, the {Cp*Ir(H)}B_4H_7 fragment. Thus, **5** is an analogue of hypothetical [{Cp*IrH}$_2$(μ,η^1-η^2-HCCH)$_2$] and a model compound for dimetal cluster assisted cyclization of two alkynes as shown in Scheme 4.

Experimental Section

General: All operations were conducted under argon atmosphere using standard Schlenk techniques. Solvents were distilled before use under N_2 as follows: sodium benzophenone ketyl for hexane, diethyl ether and tetrahydrofuran. $BH_3 \cdot THF$ (1.0 M in THF), $LiBH_4$ (2.0 M in THF), [$(Cp^*Ir)_2Cl_4$], and [$Fe_2(CO)_9$] were used as received from Aldrich. Likewise [$Co_2(CO)_8$] (Strem) was used as received. [$(Cp^*Ir)_2H_2Cl_2$] and [$(Cp^*Ir)_2HCl_3$] were prepared according to the literature procedures.[27, 52] Silica gel (60–200 mesh) was purchased from J.T. Baker Inc. and predried at 140 °C before use. Chromatography was carried out on 3 cm of silica gel in a 2.5 cm dia column. NMR spectra were recorded on a 300 MHz or 500 MHz Varian FT-NMR spectrometer. Residual proton signal of solvent was used as reference (δ, ppm, [D_6]benzene, 7.15) while a sealed tube containing [$(Me_4N)(B_3H_8)$] in [D_6]acetone (δ_B, ppm, −29.7) was used as the external reference for the ^{11}B NMR spectrum. Infrared spectra were obtained on a Nicolet 205 FT-IR spectrometer. Mass spectra were obtained on Finnigan MAT Model 8400 mass spectrometer using the EI ionization mode or the FAB mode in a 3-nitrobenzyl alcohol matrix. Perfluorokersene was used as the standard for the high resolution EI mass spectra. Elemental analysis was performed by M-H-W Laboratories, Phoenix, AZ.

Synthesis of *arachno*-[{Cp*IrH$_2$}B_3H_7] (1): In a typical reaction, [$(Cp^*Ir)_2Cl_4$] (0.10 g, 0.13 mmol) was loaded in a 100 mL schlenk tube, freshly distilled THF (6 mL) was added to generate a yellow suspension. The mixture was chilled to −40 °C and $LiBH_4$ (0.63 mmol, 0.32 mL) was added slowly by syringe. The reaction mixture was allowed to warm slowly up to room temperature. The yellow slurry turned into a green and then light yellow solution within 5 min. After the mixture had been stirred for 30 min, the THF was removed in vacuum, and the residue extracted with hexane. The ^{11}B NMR spectrum showed that there was only one boron-

  0947-6539/00/0614-2660 $ 17.50+.50/0 *Chem. Eur. J.* **2000**, *6*, No. 14

containing species. A sample of the hexane solution (1 mL) was then taken and dried. Subsequent proton NMR measurement showed two kinds of Cp* groups with approximate ratio of 1:1 (one was assigned to $[Cp^*IrH_4]$). Removal of hexane afforded a yellow oil which was sublimed at 50 °C, giving white solids containing both $[Cp^*IrH_4]$ and **1**. The white solids were then loaded in a Schlenk tube and dried under vacuum at room temperature. The colorless crystals ($[Cp^*IrH_4]$), which appeared on the upper wall, were manually removed. Crystallization of the remaining white solids in hexane gave colorless crystals (40 mg). The yield was 42 % based on the Ir. MS(FAB): *m/z*: 368 $[M-H_2]^+$, 3 B, 1 Ir atoms, calcd for weighted average of isotopomers lying within the instrument resolution, 368.1630, obsd, 368.1611; ^{11}B NMR (hexane, 22 °C): $\delta = -7.7$ (dt, $^1J(B,H) = 140$ Hz, 50 Hz, {^{1}H}, s, 1 B), −14.3 (d, $^1J(B,H) = 120$ Hz, {^{1}H}, s, 2 B); ^{1}H NMR ([D$_6$]benzene, 22 °C): $\delta = 3.11$ (pcq, 4 H, BH_t), 2.29 (pcq, 1 H, BH_t), 1.62 (s, 15 H, CH_3), −5.14 (s, br, 2 H, B-H-B), −14.51 (s, 2 H, Ir-H); IR ([D$_6$]benzene, cm^{-1}): $\tilde{\nu} = 2512$ w, 2472 m, 2420 s (B-H$_t$), 2167 m (Ir-H); elemental analysis calcd for $C_{10}H_{24}B_3Ir$: C 32.55, H 6.56; found: C 33.93, H 6.35.

Synthesis of *arachno*-[{Cp*IrH}$_2$(μ-H)BH$_4$] (2): In a typical reaction, $[(Cp^*Ir)_2H_2Cl_2]$ (0.10 g, 0.137 mmol) was loaded in a 100 mL Schlenk tube, freshly distilled toluene (5 mL) was added to generate a purple solution. $LiBH_4$ (0.2 mL, 0.4 mmol) was added at −40 °C. The −40 °C bath was then replaced with a ice-water one. The solution turned reddish brown in 10 min and the volatiles were then removed in vacuum to give a brown solid, which was extracted with hexane. The extracts were filtered through 1 cm Celite packed in a frit. The ^{11}B NMR spectrum indicated there are two major boron-containing products, **1** and **2**, plus trace amounts of **3**, while the proton NMR spectrum showed that $[Cp^*IrH_4]$ was also a co-product. The hexane solution was concentrated and kept at −40 °C for two days to give brown crystals (0.041 g). The yield was about 45 %. Note that **2** was first reported by R. G. Bergman from the reaction of $[(Cp^*Ir)_2H_3]PF_6$ with large excess of $LiBH_4$ in better yield (63 %). MS(FAB): *m/z*: 672 $[M-H_2]^+$, 1 B, 2 Ir atoms, calcd for weighted average of isotopomers lying within the instrument resolution, 672.2091, obsd, 672.2061; ^{11}B NMR (hexane, 22 °C): $\delta = 3.6$ (t, $^1J(B,H) = 110$ Hz, {^{1}H}, s, br, 1 B); ^{1}H NMR ([D$_6$]benzene, 22 °C): $\delta = 5.56$ (pcq, 1 H, B-H$_t$), 1.92 (s, 30 H, CH_3), −14.17 (s, 2 H, Ir-H-B), −17.51 (s, 1 H, Ir-H-Ir), −17.78 (s, 2 H, Ir-H$_t$); IR (hexane, cm^{-1}): $\tilde{\nu} = 2372$ m, 2298 w (B-H$_t$), 2119 m, 2044 m (Ir-H).

Synthesis of *arachno*-[{Cp*IrH}$_2$(μ-H)B$_2$H$_5$] (3): a) In a typical reaction, $[(Cp^*Ir)_2H_2Cl_2]$ (0.10 g, 0.137 mmol) was loaded in a 100 mL Schlenk tube, freshly distilled toluene (5 mL) was added to generate a purple solution. $LiBH_4$ (0.2 mL, 0.4 mmol) was added at −40 °C. The solution turned reddish brown, then brown after warming up to room temperature over 5 min. The solution was stirred for 1 h and the volatiles were then removed in vacuum to give a brown solid, which was extracted with hexane. The extracts were filtered through 1 cm Celite packed in a frit. Column chromatography was applied and elution with hexane gave a brown solution which was dried under vacuum to give brown crystals (80 mg). The yield was 85 % based on the Ir. The remaining red brown band was washed with diethyl ether. The ^{1}H NMR spectrum showed that it contained $[\{Cp^*IrH_2\}_2]$.

b) Compound **2** (0.03 g, 0.04 mmol) was dissolved in freshly distilled hexane (5 mL) in a 50 mL Schlenk tube. $BH_3 \cdot THF$ (0.08 mL, 0.08 mmol) was added at room temperature. The solution was stirred for 10 min at 50 °C. Column chromatography was applied and elution with hexane afforded a yellow solution which was dried to give brown microcrystals (0.03 mg). The ^{11}B NMR spectrum of the brown crystals showed the presence of **3** and **1** with a ratio of 3:1. The yields were 80 % and 11 % for **3** and **1**, respectively, based on the NMR data. MS(FAB): *m/z*: 684 $[M]^+$, 2 B, 2 Ir atoms, calcd for weighted average of isotopomers lying within the instrument resolution, 684.2262, obsd, 684.2259; ^{11}B NMR (hexane, 22 °C): $\delta = 14.2$ (d, $^1J(B,H) = 130$ Hz, {^{1}H}, s, 1 B), −14.6 (apparent t, s, 1 B); ^{1}H NMR: ([D$_6$]benzene, 22 °C): $\delta = 4.77$ (overlapping pcq, 1 H, B-H$_t$), 4.19 (overlapping pcq, 1 H, B-H$_t$), 2.89 (pcq, 1 H, B-H$_t$), 1.95 (s, 15 H, CH_3), 1.89 (s, 15 H, CH_3), −2.75 (s, br, 1 H, B-H-B), −13.99 (s, 1 H, Ir-H-B), −17.83 (s, 1 H, Ir-H), −17.89 (s, 1 H, Ir-H), −18.76 (s, 1 H, Ir-H); IR (hexane, cm^{-1}): $\tilde{\nu} = 2440$ m, 2389 m (B-H$_t$), 2172 w, 2102 m (Ir-H); elemental analysis calcd for $C_{20}H_{38}B_2Ir_2$: C 35.09, H 5.60; found: C 35.18, H 5.51.

Synthesis of *arachno*-[{Cp*IrH}B$_4$H$_9$] (4): Compound **1** (0.05 g, 0.14 mmol) was dissolved in THF (5 mL). An excess of $BH_3 \cdot THF$ was added and the resulting mixture was stirred at 65 °C for 20 h. Removal of hexane afforded a light yellow oil which was sublimed at 50 °C, giving white solids (45 mg). Crystallization of the remaining white solids in hexane gave colorless crystals. The yield was 88 % based on the Ir. MS(FAB): *m/z*: 380 $[M-H_2]^+$, 4 B, 1 Ir atoms. Calcd for weighted average of isotopomers lying within the instrument resolution, 380.1801, obsd, 380.1787; ^{11}B NMR (hexane, 22 °C): $\delta = -4.2$ (dt, $^1J(B,H) = 144$ Hz, 42 Hz, {^{1}H}, s, 2 B), −12.5 (t, $^1J(B,H) = 130$, {^{1}H}, s, 2B); ^{1}H NMR (C_6D_6, 22 °C): $\delta = 3.48$ (pcq, 2 H, B-H$_t$), 2.57 (pcq, 4 H, B-H$_t$), 1.59 (s, 15 H, CH_3), −4.10 (s, br, 1 H, B-H-B), −4.73 (s, br, 2 H, B-H-B), −13.11 (s, 1 H, Ir-H); IR (hexane, cm^{-1}): $\tilde{\nu} = 2118$ w, 2482 w, 2426 m (B-H$_t$); elemental analysis calcd for $C_{10}H_{25}B_4Ir$: C 31.54, H 6.62; found: C 32.67, H 6.35.

Synthesis of *arachno*-[{Cp*IrH}$_2$B$_4$H$_8$] (5): Compound **3** (0.15 g, 0.22 mmol) was dissolved in freshly distilled hexane (10 mL) in a 100 mL Schlenk tube. $BH_3 \cdot THF$ (0.88 mL, 0.88 mmol) was added at room temperature. The solution was stirred for 24 h at 60 °C. The ^{11}B NMR spectrum showed several boron-containing species, among which were the major product **5** and a second product **6**. Column chromatography was applied and elution with hexane gave a yellow solution which contains **6**. Then elution with diethyl ether gave a red solution which was slowly evaporated under nitrogen to give yellow microcrystals with some red solid. Washing with isopropanol to remove the red solid gave yellow microcrystals (**5**) (0.05 g). The yield was 32 % based on the Ir. MS(FAB): *m/z*: 708 $[M]^+$, 4 B, 2 Ir atoms, calcd for $^{12}C_{20}{}^1H_{40}{}^{11}B_4{}^{193}Ir_2$, 710.2761, obsd, 710.2809; ^{11}B NMR (hexane, 22 °C): $\delta = 34.5$ (d, $^1J(B,H) = 110$ Hz, {^{1}H}, s, 2 B), −14.7 (dd, $^1J(B,H) = 120$ Hz, {^{1}H}, s, 2 B); ^{1}H NMR (C_6D_6, 22 °C): $\delta = 6.09$ (pcq, 2 H, B-H$_t$), 3.83 (pcq, 2 H, B-H$_t$), 2.84 (pcq, 2 H, B-H$_t$), 1.67 (s, 30 H, CH_3), −1.89 (s, br, 2 H, B-H-B), −15.44 (s, 2 H, Ir-H); IR (toluene, cm^{-1}): $\tilde{\nu} = 2455$ w, 2414 m (B-H$_t$); elemental analysis calcd for $C_{20}H_{40}Ir_2B_4$: C 33.92, H 5.69; found: C 34.08, H 6.12.

Synthesis of *nido*-[1,2-{Cp*Ir}$_2$(μ-H)B$_4$H$_7$] (6): Compound **3** (0.1 g, 0.14 mmol) was dissolved in freshly distilled hexane (5 mL) in a 100 mL Schlenk tube. $BH_3 \cdot THF$ (0.56 mL, 0.56 mmol) was added at room temperature. The solution was stirred for 48 h at 65 °C. Column chromatography was applied and elution with hexane gave a yellow solution. Removal of the solvents in vacuo afforded yellow microcrystals (80 mg). The yield was 78 % based on the Ir. MS(FAB): *m/z*: 706 $[M]^+$, 4 B, 2 Ir atoms, calcd for $^{12}C_{20}{}^1H_{38}{}^{11}B_4{}^{193}Ir_2$, 708.2605, obsd, 708.2596. ^{11}B NMR (hexane, 22 °C): $\delta = 42.3$ (d, $^1J(B,H) = 150$ Hz, {^{1}H}, s, 2 B), −1.8 (d, s, $^1J(B,H) = 141$ Hz, 2 B); ^{1}H NMR ([D$_6$]benzene, 22 °C): $\delta = 6.38$ (pcq, 2 H, B-H$_t$), 3.07 (pcq, 2 H, B-H$_t$), 2.04 (s, 15 H, CH_3), 1.80 (s, 15 H, CH_3), −0.98 (s, br, 2 H, B-H-B), −4.52 (s, br, 1 H, B-H-B), −21.44 (s, 1 H, Ir-H); IR (hexane, cm^{-1}): $\tilde{\nu} = 2464$ w, 2420 m (B-H$_t$); elemental analysis calcd for $C_{20}H_{38}B_4Ir_2$: C 34.02, H 5.42; found: C 34.22, H 5.55.

Synthesis of *arachno*-[{Cp*Ir(CO)}B$_3$H$_7$] (7): Compound **1** (0.05 g, 0.14 mmol) and $[Co_2(CO)_8]$ (0.05 g, 0.15 mmol) was loaded in a 100 mL Schlenk tube. Hexane (10 mL) was added and the resulting mixture was stirred at room temperature for 10 h. Column chromatography was applied (elution with hexane). The first brown band ($[Co_4(CO)_{12}]$) was discarded and the second brown band was collected. Crystallization at −40 °C gave colorless columnlike crystals (**7**) (44 mg). The yield was 86 % based on the Ir. MS(FAB): *m/z*: 396 $[M]^+$, 3 B, 1 Ir atoms, fragment peak corresponding to loss of one CO. Calcd for weighted average of isotopomers lying within the instrument resolution, 396.1579, obsd, 396.1592. ^{11}B NMR (hexane, 22 °C): $\delta = -4.9$ (dt, $^1J(B,H) = 140$ Hz, 55 Hz, {^{1}H}, s, 1 B), −11.6 (t, $^1J(B,H) = 120$, {^{1}H}, s, 2 B); ^{1}H NMR ([D$_6$]benzene, 22 °C): $\delta = 3.21$ (overlapping pcq, 4 H, B-H$_t$), 3.10 (overlapping pcq, 1 H, B-H$_t$), 1.54 (s, 15 H, CH_3), −4.68 (s, br, 2 H, B-H-B); IR (hexane, cm^{-1}): $\tilde{\nu} = 2519$ w, 2493 w, 2435 m (B-H$_t$), 2027 vs (CO); elemental analysis calcd for $C_{11}H_{22}B_3IrO$: C 33.45, H 5.61; found: C 34.36, H 5.78.

Synthesis of *nido*-[1-{Cp*Ir}-2,3-Co$_2$(CO)$_4$(μ-CO)B$_3$H$_7$] (8): After removal of crystals of **7**, the mother liquor was concentrated and kept at −40 °C. Black platelike crystals (**8**) were produced (10 mg). The yield was 12 % based on the Ir. MS (FAB): *m/z*: 626 $[M]^+$, 3 B, 1 Ir atoms, fragment peaks corresponding to sequential loss of five CO groups. Calcd for weighted average of isotopomers lying within the instrument resolution, 626.0049, obsd, 626.0063; ^{11}B NMR (hexane, 22 °C): $\delta = 11.5$ (dt, $^1J(B,H) = 130$ Hz, 60 Hz, {^{1}H}, s, 2 B), 2.1 (d, $^1J(B,H) = 130$ Hz, {^{1}H}, s, 1 B); ^{1}H NMR ([D$_6$]benzene, 20 °C): $\delta = 4.49$ (overlapping pcq, 1 H, B-H$_t$), 4.14 (overlapping pcq, 2 H, B-H$_t$), 1.48 (s, 15 H, CH_3), −2.39 (s, br, 2 H, B-H-B), −5.39 (s, 2 H, B-H-Co); IR (hexane, cm^{-1}): $\tilde{\nu} = 2528$ w, 2472 w (B-H$_t$), 2057 s, 2025

vs, 2007 s, 1800 m (CO); elemental analysis calcd for $C_{15}H_{22}B_3Co_2IrO_5$: C 28.83, H 3.55; found: C 29.00, H 3.45.

Synthesis of *nido*-[1-{Cp*Ir}-2-Co(CO)$_3$B$_4$H$_7$] (9): Compound **4** (0.05 g, 0.13 mmol) and $[Co_2(CO)_8]$ (0.05 g, 0.15 mmol) was loaded in a 100 mL Schlenk tube. Hexane (10 mL) was added and the resulting mixture was stirred at 60 °C for 1 h. Column chromatography was applied (elution with hexane). The brown band was collected. The brown solution was kept at −40 °C overnight. Black crystals ($[Co_4(CO)_{12}]$) formed were removed by filtration. The solution was concentrated and kept at −40 °C overnight. The procedure was repeated until the solution IR indicated that there was a small amount of $[Co_4(CO)_{12}]$. Then the solution was concentrated and kept at −40 °C for several days. Large brown platelike crystals were collected (0.06 g). The yield was 90 % based on the Ir. MS(FAB): m/z: 522 $[M]^+$, 4 B, 1 Ir atoms, fragment peak corresponding to loss of three CO groups. Calcd for weighted average of isotopomers lying within the instrument resolution, 522.0903, obsd, 522.0877. ^{11}B NMR (hexane, 22 °C): $\delta = 44.2$ (d, ^1J(B,H) = 160 Hz, {^{1}H}, s, 2B), −4.3 (d, ^1J(B,H) = 155, {^{1}H}, s, 2 B); ^{1}H NMR ([D$_6$]benzene, 22 °C): $\delta = 6.22$ (q, 2H, B-H$_t$), 3.46 (q, 2H, B-H$_t$), 1.59 (s, 15H, CH$_3$), −1.02 (s,br, 2H, B-H-B), −3.62 (s, br, 1H, B-H-B); IR (hexane, cm^{-1}): $\tilde{\nu}$ = 2519 w, 2485 w (B-H$_t$), 2043 s, 1990 s, 1976 s (CO); elemental analysis calcd for $C_{13}H_{22}B_4CoIrO_3$: C 29.99, H 4.26; found: C 30.06, H 4.47.

Synthesis of *pileo*-[1-{Cp*Ir}-2,3-Co$_2$(CO)$_5$B$_3$H$_5$] (10): Compound **8** (20 mg, 0.03 mmol) was loaded in a 50 mL Schlenk tube and toluene (2 mL) was added. The solution was heated at 100 °C for 1 h. The resulting red solution was dried to afford dark red microcrystals (18 mg). The yield was 96 %. MS (FAB): m/z: 624 $[M]^+$, 3 B, 1 Ir atoms, fragment peaks corresponding to sequential loss of five CO groups. Calcd for weighted average of isotopomers lying within the instrument resolution, 623.9883, obsd, 623.9859; ^{11}B NMR (hexane, 22 °C): $\delta = 103.8$ (d, ^1J(B,H) = 160 Hz {^{1}H}, s, 1 B), 43.5 (d, ^1J(B,H) = 150 Hz, {^{1}H}, s, 1 B), 8.5 (dd, J(B,H) = 140, 70 Hz, {^{1}H}, s, 1 B); ^{1}H NMR ([D$_6$]benzene, 20 °C): $\delta = 10.22$ (pcq, 1H, B-H$_t$), 6.78 (pcq, 1H, B-H$_t$), 5.14 (pcq, 1H, B-H$_t$), 1.66 (s, 15H, CH$_3$), 1.14 (s,br, 1H, B-H-B), −3.42 (s, 2H, B-H-Co); IR (hexane, cm^{-1}): $\tilde{\nu}$ = 2498 w, 2483 w, 2459w (B-H$_t$), 2058 s, 2021 vs, 2007 m, 1998 m, 1974 m (CO); elemental analysis calcd for $C_{15}H_{20}B_3Co_2IrO_5$: C 28.93, H 3.24; found: C 29.01, H 3.22.

X-ray structure determinations

Crystallographic information for compounds **3** and **5**–**10** is given in Tables 1 and 2. Preliminary examination and data collection were performed with $Mo_{K\alpha}$ radiation ($\lambda = 0.71073$ Å) on an Enraf–Nonus CAD4 computer-controlled κ axis diffractometer equipped with a graphite crystal, incident beam monochromator at room temperature. Structure solution and refinement (based on F^2) were performed on a PC by using the SHELXTL V5 package.[53, 54] All reflections, including those with negative intensities, were included in the refinement.

***arachno*-[{Cp*IrH}$_2$(μ-H)B$_2$H$_5$] (3)**: A brown blocklike crystal, obtained by keeping a saturated hexane solution at 4 °C for several days, was mounted on a glass fiber in a random orientation. Most of the non-hydrogen atoms were located by the direct method, the remaining non-hydrogen atoms were found in succeeding difference Fourier synthesis. After all non-hydrogen atoms were refined anisotropically and hydrogen atoms of pentamethylcyclopentadienyl groups refined isotropically, difference Fourier synthesis revealed the positions for the rest of the hydrogen atoms which were refined isotropically with bond length restraints using four free variables in the refinement to confine B–H and Ir–H bond lengths around their mean values.

***arachno*-[{Cp*IrH}$_2$B$_4$H$_8$] (5)**: A yellow square pyramid-like crystal, obtained by keeping a saturated hexane solution at 4 °C for several days, was mounted on a glass fiber in a random orientation. Most of the non-hydrogen atoms were located by the direct method. The remaining non-hydrogen atoms were found in succeeding difference Fourier synthesis. After all non-hydrogen atoms were refined anisotropically and hydrogen atoms of pentamethylcyclopentadienyl groups refined isotropically, difference Fourier synthesis revealed the positions for the rest of the hydrogen atoms which were refined isotropically with bond length restraints using four free variables in the refinement to confine B–H and Ir–H bond lengths around their mean values.

Table 1. Crystallographic data and structure refinement details for compounds **3**, **5**, and **6**.

	3	**5**	**6**
empirical formula	$C_{20}H_{38}B_2Ir_2$	$C_{20}H_{40}B_4Ir_2$	$C_{20}H_{38}B_4Ir_2$
formula weight	684.52	708.16	706.14
crystal system	triclinic	tetragonal	monoclinic
space group	$P\bar{1}$	$P4_12_12$	$P2_1/n$
a [Å]	8.551(2)	8.7599(7)	8.3011(14)
b [Å]	10.306(2)	8.7599(7)	19.742(3)
c [Å]	14.884(2)	30.4203(10)	14.552(3)
α [°]	107.113(13)	90	90
β [°]	92.554(12)	90	93.448(15)
γ [°]	111.67(2)	90	90
V [Å^3]	1147.5(4)	2334.3(3)	2380.5(7)
Z	2	4	4
ρ_{calcd} [g cm^{-1}]	1.981	2.015	1.970
F(000)	644	1336	992
wavelength ($Mo_{K\alpha}$ [Å])	0.71073	0.71073	0.71073
μ [mm^{-1}]	11.585	11.392	11.171
crystal size [mm]	0.35 × 0.18 × 0.18	0.25 × 0.24 × 0.24	0.38 × 0.12 × 0.06
θ ranges [°]	2.24 to 25.01	2.42 to 24.97	2.06 to 24.98
no. of total reflns collected	4006	2054	4345
no. of unique reflns	4006 (Rint = 0.0000)	2054 (Rint = 0.0000)	4177 (Rint = 0.0330)
no of unique reflns [$I > 2\sigma(I)$]	3201	1873	3339
linear decay correction	0.7711–1.0002	0.9576–1.0223	0.9051–1.0186
abs. correction	psi-scans	XABS2	psi-scans
max. and min. transmission	1.0000, 0.7806	0.988, 0.332	0.9966, 0.8515
refinement method	full matrix on F^2	full matrix on F^2	full matrix on F^2
weighting scheme	sigma weight	sigma weight	sigma weight
data/restraints/parameters	4006/10/241	2053/7/133	4177/12/259
goodness-of-fit on F^2	1.058	1.112	1.118
R_1[a] wR_2[a] [$I > 2\sigma(I)$][a]	0.0389, 0.0963	0.0429, 0.0968	0.0382, 0.0942
R_1[a] $wR2$[b](all data)	0.0503, 0.1013	0.0498, 0.1003	0.0551, 0.1007
largest diff. peak and hole [eÅ^{-3}]	1.743, −2.196	1.082, −1.208	2.072, −1.284

[a] $R1 = \Sigma||F_o| - |F_c||/\Sigma|F_o|$. [b] $wR2 = [\Sigma w(F_o^2 - F_c^2)^2/(\Sigma w F_o^2)^2]^{1/2}$.

0947-6539/00/0614-2662 $ 17.50+.50/0 *Chem. Eur. J.* **2000**, *6*, No. 14

Table 2. Crystallographic data and structure refinement details for compounds **7**, **8**, **9**, and **10**.

	7	**8**	**9**	**10**
empirical formula	$C_{11}H_{22}B_3IrO$	$C_{15}H_{22}B_3Co_2IrO_5$	$C_{13}H_{22}B_4CoIrO_3$	$C_{15}H_{20}B_3Co_2IrO_5$
formula weight	394.92	624.82	520.68	622.80
crystal system	monoclinic	monoclinic	monoclinic	monoclinic
space group	*P*2(1)/*c*	*P*2(1)/*c*	P2(1)/c	*C*2/c
a [Å]	7.2512(4)	9.4795(4)	9.4210(6)	23.917(3)
b [Å]	14.4243(18)	9.3143(5)	16.3592(14)	23.867(3)
c [Å]	28.001(4)	23.181(2)	12.2518(9)	28.891(2)
α [°]	90	90	90	90
β [°]	97.400(10)	90.99(6)	98.846(10)	90.549(13)
γ [°]	90	90	90	90
V [Å]^3	2372.1(8)	2046.5(2)	1865.8(2)	16491(3)
Z	8	4	4	32
ρ_{calcd} [g cm^{-1}]	1.806	2.028	1.854	2.007
F(000)	1504	1192	992	9472
wavelength ($Mo_{K\alpha}$, [Å])	0.71073	0.71073	0.71073	0.71073
μ [mm^{-1}]	9.171	8.109	8.017	8.050
crystal size [mm]	0.15 × 0.15 × 0.10	0.25 × 0.25 × 0.05	0.50 × 0.38 × 0.08	0.35 × 0.25 × 0.13
θ ranges [°]	2.04 to 25.01	2.15 to 25.00	2.09 to 25.00	2.20 to 24.99
no. of total reflns collected	5239	3696	3452	14827
no. of unique reflns	5127 (*R*int = 0.0225)	3598 (*R*int = 0.0471)	3291 (*R*int = 0.0416)	14464(*R*int = 0.0330)
no of unique reflns [$I > 2\sigma(I)$]	3665	2773	2918	9570
linear decay correction	0.7086 - 1.0000	0.9336 - 1.0103	0.9488 - 1.0000	0.6992 - 1.0424
abs. correction	psi-scans	psi-scans	psi-scans	psi-scans
max. and min. transmission	1.0000, 0.6476	1.0000, 0.23765	1.0000, 0.3872	0.9967, 0.4754
refinement method	full-matrix on F^2	full-matrix on F^2	full matrix on F^2	full-matrix on F^2
weighting scheme	sigma weight	sigma weight	sigma weight	sigma weight
data/restraints/parameters	5127/20/331	3598/11/256	3291/10/220	14464/28/997
goodness-of-fit on F^2	1.042	1.062	1.069	1.032
R_1[a] wR_2[a] [$I > 2\sigma(I)$][a]	0.0475, 0.1067	0.0399, 0.1057	0.0378, 0.0978	0.0430, 0.0730
R_1[a] *wR*2[b](all data)	0.0822, 0.1324	0.0542, 0.1163	0.0430, 0.1017	0.0881, 0.0876
largest diff. peak and hole [eÅ^{-3}]	2.171, -1.169	1.617, -2.240	1.166, -1.497	0.857, -0.963

[a] $R1 = \Sigma||F_o| - |F_c||/\Sigma|F_o|$. [b] $wR2 = [\Sigma w(F_o^2 - F_c^2)^2/(\Sigma w F_o^2)^2]^{1/2}$.

***nido*-[1,2-{Cp*Ir}$_2$(μ-H)B$_4$H$_7$] (6)**: A yellow platelike crystal, obtained by keeping a saturated hexane solution at 4 °C for several days, was mounted on a glass fiber in a random orientation. Most of the non-hydrogen atoms were located by the direct method. The remaining non-hydrogen atoms were found in succeeding difference Fourier synthesis. After all non-hydrogen atoms were refined anisotropically and hydrogen atoms of pentamethylcyclopentadienyl groups refined isotropically, difference Fourier synthesis located the rest of the hydrogen atoms which were refined isotropically with bond length restraints using four free variables in the refinement to confine B–H and Ir–H bond lengths around their mean values.

***arachno*-[{Cp*Ir(CO)}B$_3$H$_7$] (7)**: Colorless columnlike crystals suitable for X-ray diffraction were obtained by keeping a saturated hexane solution at −40 °C for several days, and one was mounted on a glass fiber in a random orientation. Most of the non-hydrogen atoms were located by the direct method and the remaining non-hydrogen atoms were found in succeeding difference Fourier synthesis. Least-squares refinement was carried out on F^2 for all reflections. After all non-hydrogen atoms were refined anisotropically and hydrogen atoms of pentamethylcyclopentadienyl groups refined isotropically with riding models, difference Fourier synthesis revealed the positions for the remaining hydrogen atoms which were refined isotropically with bond length restraints using four free variables in the refinement to confine B–H distances around their mean values.

***nido*-[1-{Cp*Ir}-2,3-Co$_2$(CO)$_4$(μ-CO)B$_3$H$_7$] (8)**: Black platelike columnlike crystals suitable for X-ray diffraction were obtained by keeping a saturated hexane solution at −40 °C for several days, and one picked up in air was mounted on a glass fiber in a random orientation. Most of the non-hydrogen atoms were located by the direct method and the remaining non-hydrogen atoms were found in succeeding difference Fourier synthesis. Least-squares refinement was carried out on F^2 for all reflections. After all non-hydrogen atoms were refined anisotropically and hydrogen atoms of pentamethylcyclopentadienyl groups refined isotropically, difference Fourier synthesis revealed the positions for the remaining hydrogen atoms which were refined isotropically with bond length restraints using four free variables in the refinement to confine B–H and Co–H bond lengths around their mean values.

***nido*-[1-{Cp*Ir}-2-Co(CO)$_3$B$_4$H$_7$] (9)**: Brown platelike columnlike crystals suitable for X-ray diffraction were obtained by keeping a saturated hexane solution at −40 °C for several days, and one was mounted on a glass fiber in a random orientation. Most of the non-hydrogen atoms were located by the direct method while the remaining non-hydrogen atoms were found in succeeding difference Fourier synthesis. Least-squares refinement was carried out on F^2 for all reflections. After all non-hydrogen atoms were refined anisotropically and hydrogen atoms of pentamethylcyclopentadienyl groups refined isotropically, difference Fourier synthesis showed the positions of the remaining hydrogen atoms which were refined isotropically with bond length restraints employing four free variables in the refinement to confine B–H bond lengths around their mean values.

***pileo*-[1-{Cp*Ir}-2,3-Co$_2$(CO)$_5$B$_3$H$_5$] (10)**: Dark red polyhedronlike crystals suitable for X-ray diffraction were obtained by keeping a saturated hexane solution at −40 °C for several days, and one was mounted on a glass fiber in a random orientation. Most of the non-hydrogen atoms were located by the direct method, the remaining non-hydrogen atoms were found in succeeding difference Fourier synthesis. After all non-hydrogen atoms were refined anisotropically and hydrogen atoms of pentamethylcyclopentadienyl groups refined isotropically, difference Fourier synthesis revealed the positions for the remaining hydrogen atoms which were refined isotropically with bond length restraints employing four free variables in the refinement to confine B–H bond lengths around their mean values.

We have previously reported the structures of **3**, **5**, **6**, and **7**.[29, 30] Crystallographic data (excluding structure factors) for the structures reported in this paper have been deposited with the Cambridge Crystallographic Data Centre as supplementary publication no. CCDC-127888, CCDC-127889, and CCDC-136530–CCDC-36534. Copies of the data can be obtained free of charge on application to CCDC, 12 Union road, Cambridge CB21EZ, UK (fax:(+44) 1223-336-033; e-mail:deposit@ccdc.cam.ac.uk).

Acknowledgement

Generous support of the National Science Foundation is gratefully acknowledged. We thank Mr. D. Schifferl for aid with the NMR experiments.

[1] J. P. Collman, L. S. Hegedus, J. R. Norton, R. G. Finke, *Principles and Applications of Organotransition Metal Chemistry*, Mill Valley, CA 94941, **1987**.
[2] T. J. Marks, J. R. Kolb, *Chem. Rev.* **1977**, *77*, 263.
[3] B. D. James, M. G. H. Wallbridge, *Prog. Inorg. Chem.* **1970**, *11*, 99.
[4] Y. Nishihara, K. J. Deck, M. Shang, T. P. Fehlner, B. S. Haggerty, A. L. Rheingold, *Organometallics* **1994**, *13*, 4510.
[5] X. Lei, M. Shang, T. P. Fehlner, *J. Am. Chem. Soc.* **1998**, *120*, 2686.
[6] X. Lei, M. Shang, T. P. Fehlner, *J. Am. Chem. Soc.* **1999**, *121*, 1275.
[7] J. Ho, K. J. Deck, M. Shang, T. P. Fehlner, *J. Am. Chem. Soc.* **1995**, *117*, 10292.
[8] S. Aldridge, T. P. Fehlner, M. Shang, *J. Am. Chem. Soc.* **1997**, *119*, 2339.
[9] S. Aldridge, M. Shang, T. P. Fehlner, *J. Am. Chem. Soc.* **1998**, *120*, 2586.
[10] A. S. Weller, M. Shang, T. P. Fehlner, *Organometallics* **1999**, *18*, 53–64.
[11] A. S. Weller, M. Shang, T. P. Fehlner, *Organometallics* **1999**, *18*, 853.
[12] A. S. Weller, M. Shang, T. P. Fehlner, *Chem. Commun.* **1998**, 1787.
[13] J. D. Kennedy, *Prog. Inorg. Chem.* **1984**, *32*, 519.
[14] J. D. Kennedy, *Prog. Inorg. Chem.* **1986**, *34*, 211.
[15] J. Bould, N. N. Greenwood, J. D. Kennedy, W. S. McDonald, *J. Chem. Soc.*, *Dalton Trans.* **1985**, 1843.
[16] S. K. Boocock, M. A. Toft, K. E. Inkrott, L.-Y. Hsu, J. C. Huffman, K. Folting, S. G. Shore, *Inorg. Chem.* **1984**, *23*, 3084.
[17] J. Bould, N. N. Greenwood, J. D. Kennedy, *J. Chem. Soc.*, *Dalton Trans.* **1982**, 481.
[18] N. N. Green, J. D. Kennedy, W. S. McDonald, D. Reed, J. Staves, *J. Chem. Soc. Dalton Trans.* **1979**, 117.
[19] J. Bould, N. P. Rath, L. Barton, *Organometallics* **1995**, *14*, 2119.
[20] J. Bould, M. Pasieka, J. Braddock-Wilking, N. P. Rath, L. Barton, C. Gloeckner, *Organometallics* **1995**, *14*, 5138.
[21] J. Bould, N. P. Rath, L. Barton, *J. Chem. Soc. Chem. Commun.* **1995**, 1285.
[22] J. Bould, N. P. Rath, L. Barton, *Inorg. Chem.* **1996**, *35*, 35.
[23] J. Bould, N. P. Rath, L. Barton, *Chem. Commun.* **1995**, 1285.
[24] J. Bould, N. P. Rath, L. Barton, *Angew. Chem.* **1995**, *107*, 1744; *Angew. Chem. Int. Ed. Engl.* **1995**, *34*, 1641.
[25] J. Bould, N. P. Rath, H. Fang, L. Barton, *Inorg. Chem.* **1996**, *35*, 2062.
[26] S. L. Shea, T. D. McGrath, T. Jelinek, B. Stibr, M. Thornton-Pett, J. D. Kennedy, *Inorg. Chem. Comm.* **1998**, *1*, 97.
[27] C. White, A. J. Oliver, P. M. Maitlis, *J. Chem. Soc. Dalton Trans.* **1973**, 1901.
[28] T. M. Gilbert, F. J. Hollander, R. G. Bergman, *J. Am. Chem. Soc.* **1985**, *107*, 3508.
[29] X. Lei, A. K. Bandyopadhyay, M. Shang, T. P. Fehlner, *Organometallics* **1999**, *18*, 2294.
[30] X. Lei, M. Shang, T. P. Fehlner, *Organometallics* **2000**, *19*, 118.
[31] T. M. Gilbert, R. G. Bergman, *Organometallics* **1983**, *2*, 1458.
[32] X. Lei, M. Shang, T. P. Fehlner, *Organometallics* **1998**, *17*, 1558.
[33] J. Bould, J. D. Kennedy, W. S. McDonald, *Inorg. Chim. Acta* **1992**, *196*, 201.
[34] L. J. Guggenberger, A. R. Kane, E. L. Mutterties, *J. Am. Chem. Soc.* **1972**, *94*, 5665.
[35] B. S. Haggerty, C. E. Housecroft, A. L. Rheingold, B. A. M. Shaykn, *J. Chem. Soc. Dalton Trans.* **1991**, 2175.
[36] C. E. Housecroft, S. M. Owen, P. R. Raithby, B. A. M. Shaykn, *Organometallics* **1990**, *9*, 1617.
[37] C. E. Housecroft, B. A. M. Shsykn, A. L. Rheingold, B. S. Haggerty, *Inorg. Chem.* **1991**, *30*, 125.
[38] A. R. Kane, E. L. Mutterties, *J. Am. Chem. Soc.* **1971**, *93*, 1041.
[39] N. N. Greenwood, J. D. Kennedy, D. Reed, *J. Chem. Soc. Dalton Trans.* **1980**, 196.
[40] W. D. Jones, R. M. Chin, *J. Am. Chem. Soc.* **1994**, *116*, 198.
[41] J. Feilong, T. P. Fehlner, A. L. Rheingold, *J. Organomet. Chem.* **1988**, *348*, C22.
[42] R. Ahmad, J. E. Crook, N. N. Greenwood, J. D. Kennedy, *J. Chem. Soc. Dalton Trans.* **1986**, 2433.
[43] K. J. Deck, Y. Nishihara, M. Shang, T. P. Fehlner, *J. Am. Chem. Soc.* **1994**, *116*, 8408.
[44] S. Ghosh, M. Shang, T. P. Fehlner, *J. Am. Chem. Soc.* **1999**, *121*, 7451.
[45] R. L. Thomas, L. Barton, *Inorg. Chem. Acta* **1999**, *289*, 134.
[46] J. Bould, N. N. Greenwood, J. D. Kennedy, *J. Chem. Soc. Dalton Trans.* **1984**, 2477.
[47] X. Lei, M. Shang, T. P. Fehlner, *Inorg. Chem.* **1998**, *37*, 3900.
[48] K. B. Gilbert, S. K. Boocock, S. G. Shore in *Comprehensive Organometallic Chemistry*, *Vol. 5* (Eds: G. Wilkinson, F. G. A. Stone, E. Abel), Pergamon, Oxford, **1982**, p. 879.
[49] J. P. Collman, J. W. Kang, W. F. Little, M. F. Sullivan, *Inorg. Chem.* **1968**, *7*, 1298.
[50] G. M. Whitesides, W. J. Ehmann, *J. Am. Chem. Soc.* **1969**, *94*, 3800.
[51] D. R. McAlister, J. E. Bercaw, R. G. Bergman, *J. Am. Chem. Soc.* **1977**, *99*, 1666.
[52] D. S. Gill, P. M. Maitlis, *J. Organomet. Chem.* **1975**, *87*, 359.
[53] G. M. Sheldrick, University of Göttingen, **1997**.
[54] SHELXTL Version 5, Siemens Industrial Automation Inc. **1994**.

Received: November 8, 1999 [F2122]

  0947-6539/00/0614-2664 $ 17.50+.50/0